Kinematic analysis of shear displacement as a means for operating mechanotransduction channels in the contact region between adjacent stereocilia of mammalian cochlear hair cells

DAVID N. FURNESS[1]*, DEBORAH E. ZETES[2], CAROLE M. HACKNEY[1] AND CHARLES R. STEELE[2]

[1] *Department of Communication and Neuroscience, Keele University, Keele, Staffordshire, ST5 5BG, UK*
[2] *Department of Mechanical Engineering, Stanford University, Stanford, CA, 94305, USA*

SUMMARY

In sensory hair cells of the cochlea, deflection of the stereociliary bundle results in direct mechanical gating of mechanoelectrical transduction channels, a function generally attributed to the tip link running between the tips of short stereocilia and the sides of adjacent taller ones. However, immunocytochemical experiments indicate that the channels may not be associated with the tip link but occur just below it in a region of contact between the stereocilia. To determine whether transduction channels in this location could be operated during physiologically appropriate deflections as effectively by shear displacement as if they were associated with the tip link, a two-dimensional kinematic analysis of relative motion between stereocilia has been performed assuming contact between stereocilia is maintained during deflection. Bundle geometry and dimensions were determined from transmission electron micrographs of hair cells from several frequency locations between 0.27 and 13.00 kHz in the guinea-pig cochlea. The analysis indicates that for a 10 nm deflection of the tallest stereocilia of both inner and outer hair cells, i.e. within the range of the maximum sensitivity of mammalian hair bundles, the average shear displacement in the contact region would be 1.6 nm, but that it increases systematically towards higher frequency regions for outer hair cells. This displacement is comparable in magnitude to tip-link elongation for individual stereociliary pairs.

1. INTRODUCTION

The mechanosensitive hair cells of the vertebrate acousticolateral system possess an apical bundle of stereocilia arranged in rows of increasing height. These stereocilia are interconnected by two types of extracellular cross links, the lateral links (Flock *et al*. 1977) which run between the stereociliary shafts, and the tip links which run between the tips of each short stereocilium and the sides of the taller ones behind (Osborne *et al*. 1984; Furness & Hackney 1985). The stereocilia contain an actin core and behave like stiff rods, pivoting around their insertions into the cell when their distal ends are deflected (Flock *et al*. 1977). Deflection of the bundle towards the tallest row of stereocilia causes an increased probability of opening of cationic channels (Corey & Hudspeth 1979*a*) producing depolarization of the hair cell, whilst deflections in the opposite direction lead to hyperpolarization. The short time constants of receptor currents imply that the operation of the channels must be purely mechanical (Corey & Hudspeth 1979*b*; Crawford *et al*. 1989) leading to the suggestion that each channel is directly opened by a 'gating spring' (see Howard *et al*. 1988 for a review). It has been proposed that the tip links are suitably placed for this function; positive deflections would increase tension in them whilst negative deflections would reduce tension, thus accounting for the polarization of the hair-cell response (Osborne *et al*. 1984). However, immunocytochemical experiments aimed at localizing the transduction channels have suggested that they may occur just below the tip links and above the lateral links, at the point where the shorter stereocilia come into closest proximity with the taller stereocilia. Membrane specializations have been observed in this contact region in both mammalian (Hackney *et al*. 1992) and reptilian hair bundles (Hackney *et al*. 1993).

Two recent models of the rearrangement of the stereocilia during deflection of the hair bundle have specifically compared the elongation of the tip and lateral links, and suggested that the tip links are more appropriately placed for operating the transduction channels (Geisler 1993; Pickles 1993). However, neither of these models used relevant geometry or dimensions to provide information about the contact

* Author to whom correspondence should be addressed.

region. To determine whether transduction channels in this location could be operated as effectively by shear displacement as by tip-link elongation, a two dimensional geometric analysis of relative motion of the stereocilia has been performed. For this kinematic analysis, geometry and dimensions have been obtained from electron microscopy of hair bundles from the guinea-pig cochlea. These have been used to calculate the ratio between deflection of the tip of the tallest stereocilium and shear displacement at the contact region during deflections and, for comparison, the elongation of the tip and lateral links. Because the mammalian cochlea has two types of hair cell, one row of inner hair cells (IHCs) and three rows of outer hair cells (OHC1–OHC3), and the height and organization of bundles varies with type, row and location (e.g. Lim 1986), examples of all rows have been analysed from different frequency locations.

2. METHODS

(*a*) *Preparation for electron microscopy*

Two guinea-pigs (450 g and 845 g) were killed with an overdose of sodium pentobarbitone (400 mg kg^{-1}, IP), decapitated, and the bullae opened. The cochleas were gently perfused with 2.5% (by volume) glutaraldehyde in 0.1 M sodium cacodylate buffer (pH 7.4) containing 2 mM $CaCl_2$ via holes made in the apex and the round and oval windows. They were immersed in this fixative for 2 h, washed in buffer, and post-fixed for 1 h in 1% OsO_4 (by weight) in the same buffer. One pair were prepared for scanning electron microscopy (SEM) by removal of the bony shell and further impregnation with osmium by immersing them twice for 1 h in 1% (by weight) OsO_4 alternating with 20 min in a saturated aqueous solution of sodium thiocarbohydrazide interspersed by thorough washing in distilled water. They were dehydrated via an ethanol series, critical-point dried using carbon dioxide as the transitional fluid, and then glued to a stub using electroconductive silver paint (Agar Scientific) prior to observation in a Hitachi S-4500 field emission scanning electron microscope operated at an accelerating voltage of 2 kV.

The shells of the remaining cochleas were partially removed and each was dehydrated via a series of ethanols, embedded whole in Durcupan resin (Fluka) and microsliced into hemicoils (Jiang *et al.* 1993). The hooks were trimmed into smaller segments to minimize errors due to estimation of a non-planar arc length. The resultant hemicoils and segments were photographed with a light microscope to measure the length of the organ of Corti.

Ultrathin sections were cut in the radial plane from locations for which the best frequency was estimated using Greenwood's function (Greenwood 1990), collected onto copper grids, stained using uranyl acetate and lead citrate and examined in a JEOL 100CX transmission electron microscope operated at 100 kV. Hemicoils were remeasured after sectioning to determine the precise location from which the ultrathin sections had been taken.

(*b*) *Stereociliary measurements*

Micrographs containing longitudinal sections of the stereocilia were taken at magnifications of X8300 and X13000 by transmission electron microscopy (TEM) and the magnifications calibrated in each observation session by photographing a grating with 2160 lines mm^{-1} (Agar Scientific). Stereociliary height measurements were made from the distal tip to the centre of the rootlet, only when the rootlet and the dense cap which occurs at the tip (e.g. Furness & Hackney 1985) were both visible, to minimize errors caused by an oblique section plane. The spacing between the bases of stereocilia in adjacent rows was measured from the centre of each rootlet. The angle made by each stereocilium with the hair cell apex was measured between the line along the long axis of the stereocilium and the line which best fitted the apical surface by eye. The strict application of these criteria meant that large numbers of sections were required to obtain measurements, especially from hair bundles with long stereocilia such as the IHCs. The positions of tip-link and lateral-link attachments were also measured in a section of a pair of stereocilia in which these links were completely visible and in which the other dimensions were also obtainable.

3. RESULTS

(*a*) *Hair bundle morphology and measurements*

Examination of complete hair bundles in SEM, and thin sections in TEM, shows that stereocilia from adjacent rows are inclined towards each other (figures 1*a* & 2*a*). At the contact region, the membranes of the shorter stereocilia approach to within 3 nm of the sides of the taller stereocilia (figure 2*b*) whilst the rootlets are approximately 200 nm apart, so that a triangle is formed between the hair cell apex and the short and tall stereocilia (figure 2*a*). The region in which the stereocilia come into contact lies in a similar plane to the tip links, approximately 100–200 nm below their attachment to the shorter stereocilium and 200–300 nm closer to the stereociliary tip than the lateral links (figures 1*b* & 2*b*).

Average values for stereociliary length, angle and rootlet spacing have been obtained from seven different frequency locations for OHCs, and from six locations for IHCs. These show that in all three rows of OHCs, the lengths of the tallest stereocilia decrease significantly with frequency. The change in length for the three rows of OHCs is, however, substantially different; OHC1 shows a 1.8× change over the frequency range measured, OHC2 a 2.6× change and OHC3 a greater than 3.0× change (table 1). Thus, although similar in the high frequency regions, the lengths of the tallest stereocilia differ considerably in the low frequency regions. For IHCs, although the length of the tallest stereocilia in the low frequency region is 1.5× that in the high frequency region, no significant correlation between length and frequency region could be detected for the low numbers of hair bundles analysed.

The OHCs have three rows of stereocilia in all cases except for OHC2 and OHC3 in the 0.27 and 0.36 kHz regions which have only two. The IHCs often have four rows, but for comparison with the OHCs and because the fourth row shows substantial variation in organization, only the first three rows have been considered here. Rootlet spacings between the first and second rows (pair 1) and between the second and third rows (pair 2) do not change significantly with frequency for any of the hair cell types. In OHCs, there are no significant differences between the rootlet spacings for pair 1 (mean 0.41 μm ± 0.05 (SD), n = 95) and pair 2 (0.43 μm ± 0.08, n = 71), but in IHCs

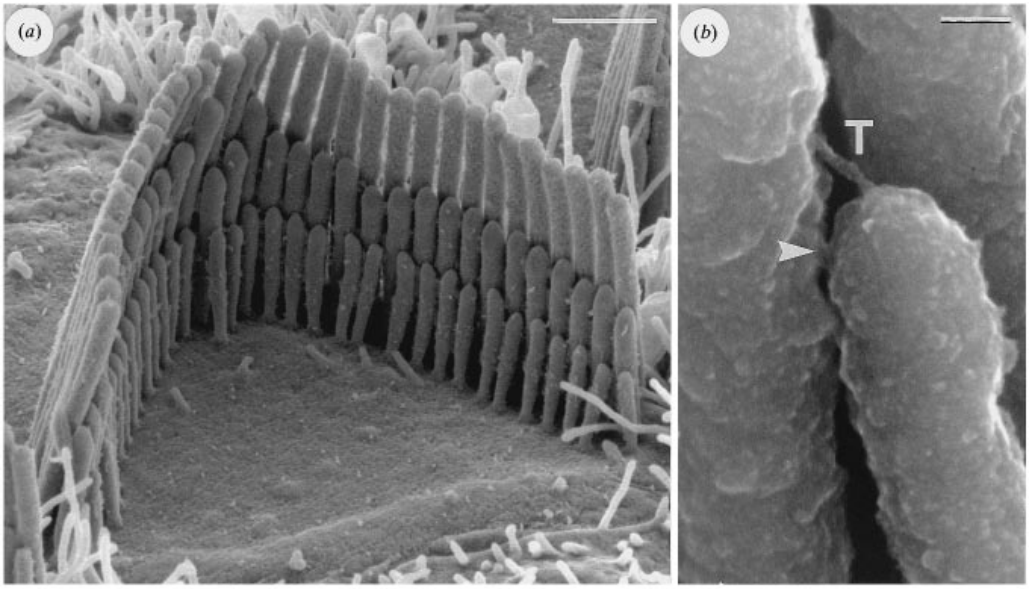

Figure 1. (*a*) SEM of the stereociliary bundle of an outer hair cell. Note that the rows of stereocilia lean towards one another. Scale bar = 1 μm. (*b*) Detail of the contact region (arrowhead) and the tip link (T) from an inner hair cell. Scale bar = 50 nm.

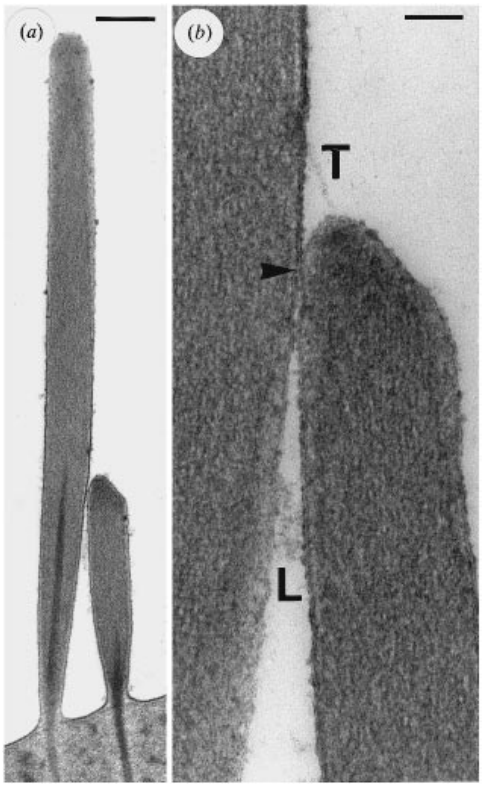

Figure 2. (*a*) TEM of a longitudinal section showing the triangle formed between stereocilia from adjacent rows in an outer hair cell. Scale bar = 0.4 μm. (*b*) Higher magnification view of the contact region (arrowhead), lateral links (L), and tip link (T). Scale bar = 100 nm.

the spacing for pair 1 (0.60 μm ± 0.09, $n = 13$) is significantly greater than for pair 2 (0.37 μm ± 0.07, $n = 13$; $p < 0.001$, Wilcoxon sign-rank test).

The tallest OHC stereocilia are nearly always inclined towards the shorter rows, with angles from the vertical ranging between +9° and −23° (where negative values represent inclination in the direction of the shorter rows). The mean angle for OHC1 is −8° ± 7, for OHC2, −13° ± 4, and for OHC3 −12° ± 6. In IHCs, the angle ranges between +20° and −12°, with a mean of −4° ± 9, although the apical surface of these cells is often considerably curved, making measurement of the angle more difficult than for OHCs.

(*b*) *Kinematic analysis*

Although hair bundles have a variable number of stereociliary rows, for clarity this analysis will consider the relative planar movement between two stereocilia of adjacent rows, the geometry of which is illustrated in figure 3. Equations for additional rows can be derived similarly with sequential solution of the equations and repeated application of the chain rule (Zetes 1995).

This analysis considers the constraint that the stereocilia remain in contact throughout bundle deflection such that the stereociliary surfaces slide relative to each other whilst rotating about their attachments to the cuticular plate at points OA and OB on the tall and the short stereocilium respectively. For enforcement of this constraint the stereociliary contours must be written analytically. The radius of curvature of the cap of the short stereocilium varies continuously from the radius of the shaft to a small local radius at its most apical point (figure 2*b*). However, for small deflections of the stereocilia, movement of the contact point between stereociliary pairs is small. The radius of curvature of the cap at this point is therefore approximated by the maximum radius of the shaft. The angular deflection of the short stereocilium, θ_B, is then related to that of the tall stereocilium, θ_A, by

$$\theta_B = \theta_A - \mathrm{Arcsin}\left(\frac{c - a\cos\theta_A}{b}\right), \qquad (1)$$

Table 1. *Stereociliary lengths and shear ratios in hair bundles from different frequency locations*

(The average lengths of the tallest stereocilia are shown (±confidence limits calculated where possible given the small sample sizes (n) using Student's t), and the shear ratios for the first (pair 1) and second (pair 2) pair of stereocilia for each hair cell type in each frequency location. Where no shear ratio is given for pair 2, bundles contained only two rows of stereocilia. Stereociliary heights decrease significantly with increasing frequency in all three OHC rows (Spearman's rank correlation (r_s), $p < 0.01$) but not in IHCs. The shear ratios for OHCs are also correlated with frequency (r_s for OHC1, pairs 1 & 2, OHC2, pair 2, $p < 0.05$; for OHC2, pair 1 and OHC3, pairs 1 & 2, $p < 0.01$). For IHCs, there is no correlation of shear ratio with frequency. Means and standard deviations of the shear ratio for each hair cell type are given in the text. (This table includes data from Zetes 1995.))

hair cell type	frequency region (kHz)	length (μm) of tall stereocilium	shear ratio	
			pair 1	pair 2
IHC	0.27	5.3±0.8 (6)	0.11	0.07
	0.36	4.3 (1)	0.18	0.11
	1.08	3.9±0.3 (6)	0.13	0.11
	2.03	3.9±0.2 (3)	0.16	0.08
	4.50	4.0 (1)	0.16	0.12
	13.00	3.5 (2)	0.17	0.09
OHC1	0.27	2.9±0.1 (6)	0.16	0.16
	0.36	2.5±0.2 (5)	0.16	0.18
	0.61	2.2±0.5 (2)	0.21	0.24
	1.08	2.2±0.0 (3)	0.16	0.17
	2.03	2.1±0.2 (6)	0.20	0.23
	4.50	1.9±0.5 (4)	0.22	0.31
	13.00	1.6±2.0 (2)	0.28	0.28
OHC2	0.27	4.6±1.8 (2)	0.10	—
	0.36	3.9±0.7 (3)	0.11	—
	0.61	3.6±1.6 (2)	0.12	0.13
	1.08	3.2±0.2 (9)	0.11	0.09
	2.03	2.3±0.1 (4)	0.18	0.20
	4.50	2.1±0.3 (4)	0.20	0.24
	13.00	1.7±0.2 (5)	0.25	0.32
OHC3	0.27	5.6 (1)	0.10	—
	0.36	5.1±1.6 (2)	0.08	—
	0.61	4.8±0.4 (3)	0.08	0.08
	1.08	4.3±0.3 (10)	0.09	0.09
	2.03	3.2±3.5 (2)	0.12	0.12
	4.50	2.2±0.2 (4)	0.20	0.16
	13.00	1.7±0.8 (2)	0.23	0.24

where a is the distance between the rootlets, b is the distance between the centre of curvature of the cap of the shorter stereocilium and its intersection with the apical surface, and c is the sum of the radii of the two stereocilia. The location, s, of the contact point, AB, is determined by the orthogonal projection along the central axis of the tall stereocilium of a line drawn from OA to AB and is given by

$$s = b\cos(\theta_A - \theta_B) - a\sin\theta_A. \quad (2)$$

Combining equations (1) and (2), the angle θ_B can be eliminated to give

$$s = b\left[1 - \left(\frac{c - a\cos\theta_A}{b}\right)^2\right]^{\frac{1}{2}} - a\sin\theta_A. \quad (3)$$

For comparison with physiological experiments, the angle θ_A is related to the horizontal distance of the tip of the tall stereocilium at point XA from the normal of the apical surface through point OA by the relationship

$$x = L\sin\theta_A, \quad (4)$$

where L is the length of the tall stereocilium.

The dependence of the location of the contact point on the horizontal deflection of the tip of the tall stereocilium can be studied by considering a shear ratio κ, defined as the negative of the partial derivative of the location of the contact point, s, with respect to the horizontal location of the tip of the tall stereocilium, x. By equation (4), the shear ratio can also be written as a derivative with respect to the angular rotation of the tall stereocilium, θ_A, as follows

$$\kappa \equiv -\frac{\partial s}{\partial x} = -\frac{1}{L\cos\theta_A}\frac{\partial s}{\partial \theta_A} \qquad -\frac{\pi}{2} \leqslant \theta_A \leqslant \frac{\pi}{2}. \quad (5)$$

Performing the differentiation explicitly, the shear ratio is given by

$$\kappa = \frac{a}{L} + \frac{a}{L}\left(\frac{c - a\cos\theta_A}{b}\right)\left[1 - \left(\frac{c - a\cos\theta_A}{b}\right)^2\right]^{-\frac{1}{2}}\tan\theta_A$$

$$-\frac{\pi}{2} \leqslant \theta_A \leqslant \frac{\pi}{2}. \quad (6)$$

This definition of the shear ratio (5) is effectively a linearization of the shear displacement with respect to tip deflection about a non-zero nominal solution. The resulting relationship (6) is a function of the nominal angle, θ_A, which can be relatively large (e.g. 23°) in comparison with the changes of angle for physiologically reasonable deflections which are small (< 1°) (Howard *et al.* 1988).

In the limit for small ratios c/b and a/b, equation (1) approaches to $\partial\theta_A/\partial\theta_B = 1$ which reduces to the result for parallel slender stereocilia (Geisler 1993). For inclined stereocilia, as shown in figure 1, this condition is not satisfied when enforcing a contact constraint and $\partial\theta_A/\partial\theta_B < 1$. In the same limit, equation (6) reduces to $\kappa = a/L$. However, if the second row becomes substantially shorter or the rootlets become more widely spaced relative to the length of the tallest stereocilium, the shear ratio becomes dependent on the angular orientation of the rows as seen by inspection of equation (6).

(*c*) *Numerical evaluation*

Shear ratios have been calculated using the average measurements obtained for each frequency region (table 1). The shear ratio for OHCs ranges from 0.08 to 0.32, with a mean of 0.16 (±0.06). Thus for a deflection of 10 nm the shear displacement, ∂s, defined as the resultant change in the location of the contact point along the tall stereocilium, varies between 0.8 and 3.2 nm. There are no significant differences between the means for the two pairs of stereocilia, either within a row of OHCs or between the OHC rows. However, the shear ratio increases significantly with frequency for both stereociliary pairs in all three rows of OHCs. This change means that a constant

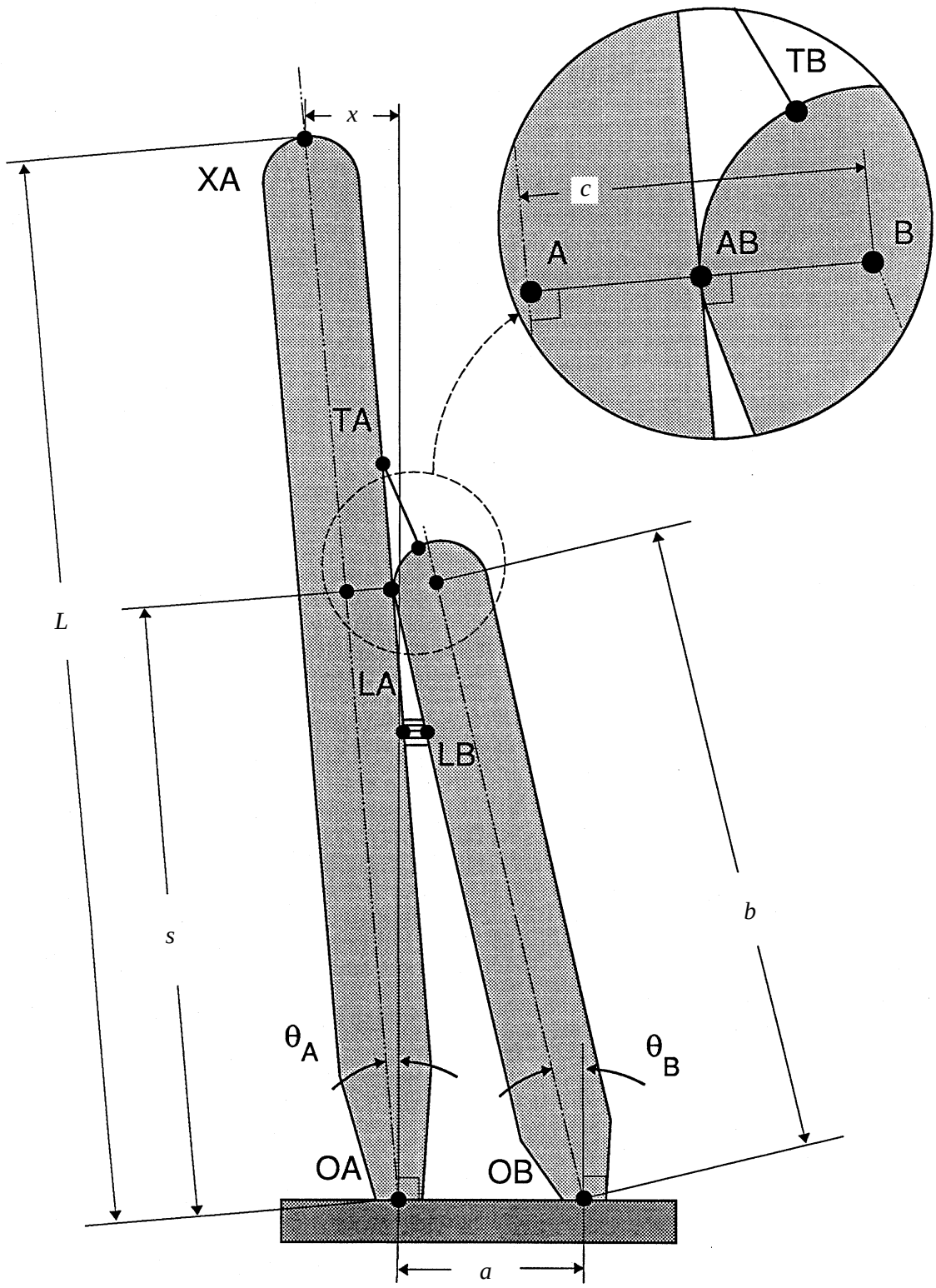

Figure 3. Schematic diagram of a pair of stereocilia (main diagram) and the tip region (inset) illustrating the geometrical parameters used in the analysis. The tall and short stereocilia are attached to the cuticular plate by hinges at points OA and OB respectively and are in contact at point AB. Point B is the centre of curvature of the upper cap of the short stereocilium. Point A is located at the intersection of a perpendicular line drawn from point B to the long axis of the stereocilium. The tip link attaches at points TA on the taller stereocilium and TB on the shorter stereocilium and the lateral links at LA and LB, respectively. Point XA, at the tip of the tallest stereocilium, denotes the location for the expression of the horizontal distance x, of point XA from the normal to the apical surface through OA. The angles of the tall and short stereocilia relative to the normal of the apical surface, θ_A and θ_B respectively, and the tip deflection x, are positively defined as drawn.

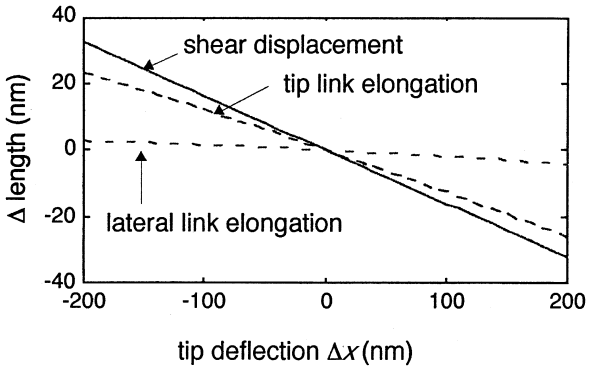

Figure 4. Shear displacement, tip-link elongation, and lateral-link elongation versus tip deflection for a typical stereociliary pair. For small deflections, all three calculated quantities show a linear relationship with tip deflection. The shear displacement and the elongation of the tip links are of the same order, whilst lateral-link elongation is an order of magnitude smaller. The values used for this calculation were as follows: $L = 4.43$ μm; $a = 0.45$ μm; $b = 1.45$ μm; $c = 0.30$ μm; $\theta_A = -10°$.

angular rotation, rather than a constant tip deflection, gives similar shear displacements at the contact region in OHCs at the different frequency locations, being 7.2 nm ± 0.61 (mean ± SD) for pair 1 and 7.6 nm ± 1.2 for pair 2 for a rotation of 1°.

In IHCs, the shear ratio ranges from 0.07 to 0.18 and is not significantly correlated with frequency. However, it differs significantly between pair 1 (0.15 ± 0.03) and pair 2 (0.09 ± 0.02; $p < 0.05$, Wilcoxon sign-rank test).

Shear displacement in the contact region has also been compared with elongation of the tip and lateral links over a range of physiologically appropriate deflections for a single pair of stereocilia for which all the appropriate measurements could be obtained. From this, it can be seen that the elongation of the tip link, ∂t, calculated as the change in distance between points TA and TB under the contact constraint is less than the shear displacement although they are of the same order of magnitude (figure 4). The elongation of the lateral links, ∂l, calculated as the change in distance between points LA and LB is, however, an order of magnitude smaller.

4. DISCUSSION

The morphological data presented here confirm that the contact region located below the tips of the mammalian stereocilia is distinct from the lateral links and show that it is the only place where their membranes come into direct contact. This, coupled with the possible immunolocalization of the transduction channels in this region, makes it relevant to explore the relative movement of stereocilia at this point in a way that has not been attempted in previous models. The analysis differs from that of Geisler (1993) in two ways; first, it takes account of the inclination of the stereocilia relative to the apical surface of the cell, which becomes larger for higher frequency bundles and for shorter rows. Secondly, it enforces a contact constraint in accordance with recent experimental observations which show that the stereocilia remain closely opposed during both static and quasi-static deflections of the bundle (Corey *et al.* 1989; Duncan *et al.* 1994).

The present work also differs from that of Jacobs & Hudspeth (1990) in which measurements of stereociliary bundle width were made and divided by the number of rows to give an average separation. The ratio between this and the bundle height was then taken to obtain the geometric gain. This latter method would not provide an appropriate approximation for mammalian bundles in which there are few stereociliary rows and substantial differences in height between them and also could not be used to compare rows within a bundle.

The kinematic analysis was performed using average geometric parameters for the lengths, angulation and separation of different stereociliary rows from OHCs and IHCs in different frequency locations. These measurements confirm that for OHCs the lengths of the tallest stereocilia decrease progressively towards the high frequency region of the cochlea, as reported by others for several different vertebrate classes and species (Lim 1986; Fettiplace 1990). However, the rootlet separations remain constant and do not differ significantly between rows of stereocilia.

For the IHCs the situation is less clear; whilst there does not appear to be a significant correlation between length and frequency, the tall stereocilia are clearly shorter in the highest frequency region than the lowest frequency region analysed. The lack of correlation may simply reflect the relatively small sample of IHC measurements obtained here. There is, however, a significant difference in rootlet spacing between the first and second pairs of stereocilia that is seen in all frequency regions.

Shrinkage or deformation caused by the preparation technique may affect the measurements compared with the *in vivo* state. However, unless shrinkage occurs disproportionately in different cochlear regions or hair cell types, the observed systematic variations in stereociliary length in OHCs compared with IHCs could not have arisen artifactually. In addition, provided shrinkage is uniform for different cellular compartments such as the stereocilia and cuticular plates, the calculated shear ratios would not be affected.

The change in stereociliary length coupled with the constant rootlet separation result in a gradual change in geometry in OHCs. This produces a systematic increase in shear ratio with increasing frequency for both pairs of stereocilia. Assuming that the shear displacement is being used to operate transduction channels, then the increase in shear ratio with decreasing length means that the sensitivity of the hair cells to tip deflection increases as the stereocilia become shorter, as suggested previously by Fettiplace (1990). However, for a given angular rotation of the tallest OHC stereocilia, the rate at which the change occurs means that a relatively constant shear displacement will be obtained between the adjacent stereocilia.

Similarly, the lack of a significant systematic change of shear ratio with frequency in IHCs is consistent with

the poor correlation between lengths of the tallest stereocilia and frequency in the present measurements. Nevertheless, although the curvature of the IHC apex makes accurate measurement more difficult, the shear ratio for the first pair is significantly larger than for the second, as a consequence of differences in rootlet spacing and angulation.

Whilst the present analysis has revealed a systematic change in shear ratio with frequency, the same relationship could also be observed for the taller pair of stereocilia using the approximation a/L, obtained from equation (6). Mean values calculated using a/L for OHCs (0.16 ± 0.03) and IHCs (0.15 ± 0.06) are, in fact, identical to those calculated from the kinematic analysis. The method used by Jacobs & Hudspeth (1990) also produced a similar value for bullfrog saccular hair bundles (0.14). However, the approximation of this method becomes increasingly less valid for shorter, non-parallel stereocilia, and therefore would not have revealed the difference between IHC pairs. Thus the complete solution (6) is required for higher frequency cells where angulation becomes greater. Further, more accurate analysis including the kinetics of the linkages and stereocilia, could also be considered.

The analysis has also been used to compare shear displacement in the contact region with tip-link and lateral-link elongation in an individual stereociliary pair. The shear displacement is found to be greater than tip-link elongation as would be predicted from the fact that the tip link is inclined with respect to the axis of the taller stereocilium whilst the relative displacement occurs parallel to the axis. The two are, however, similar in magnitude but an order of magnitude greater than lateral-link elongation. This confirms that the lateral links observed below the contact region would not be an effective means of operating the channels, as concluded by Pickles (1993) and Geisler (1993). However, Geisler showed that when horizontal connections between the stereocilia are less than 16 nm long, the sensitivity of these structures to deflections approaches that of the tip link. Thus, the pillar-like horizontal connections which appear to cross both membranes of the stereocilia in the contact region (Hackney & Furness 1995) where the membranes are less than 3 nm apart, could be effective channel-gating elements according to Geisler's analysis. This accords with the present analysis which shows that channels located in the contact region could be operated as efficiently as if they were at the ends of tip links.

This work was supported by grants from the Wellcome Trust and Hearing Research Trust to C.M.H. and D.N.F., and NIH Grant No. R01 DC00108 to C.S.

REFERENCES

Corey, D. P., Hacohen, N., Huang, P. L. & Assad, J. A. 1989 Hair cell stereocilia bend at their bases and touch at their tips. *Soc. Neurosci. Abstr.* **15**, 208a.

Corey, D. P. & Hudspeth, A. J. 1979*a* Ionic basis of the receptor potential in a vertebrate hair cell. *Nature, Lond.* **281**, 675–677.

Corey, D. P. & Hudspeth, A. J. 1979*b* Response latency of vertebrate hair cells. *Biophys. J.* **26**, 499–506.

Crawford, A. C., Evans, M. G. & Fettiplace, R. 1989 Activation and adaptation of transducer currents in turtle hair cells. *J. Physiol., Lond.* **419**, 405–434.

Duncan, R. K., Hernandez, H. N. & Saunders, J. C. 1995 Relative stereocilia motion on chick hair cells during high frequency stimulation. *Association for Research in Otolaryngology, abstracts of the eighteenth midwinter research meeting* No. **634**, 159.

Fettiplace, R. 1990 Transduction and tuning in auditory hair cells. *Semin. Neurosci.* **2**, 33–40.

Flock, Å., Flock, B. & Murray, E. 1977 Studies on the sensory hairs of receptor cells in the inner ear. *Acta Otolaryngol.* **83**, 85–91.

Furness, D. N. & Hackney, C. M. 1985 Cross-links between stereocilia in the guinea-pig cochlea. *Hear. Res.* **18**, 177–188.

Geisler, C. D. 1993 A model of stereociliary tip-link stretches. *Hear. Res.* **65**, 79–82.

Greenwood, D. D. 1990 A cochlear frequency-position function for several species – 29 years later. *J. Acoust. Soc. Am.* **87**, 2592–2605.

Hackney, C. M. & Furness, D. N. 1995 Mechanotransduction in vertebrate hair cells: structure and function of the stereociliary bundle. *Am. J. Physiol.* **268**, C1–C13.

Hackney, C. M., Furness, D. N., Benos, D. J., Woodley, J. F. & Barratt, J. 1992 Putative immunolocalization of the mechanoelectrical transduction channels in mammalian cochlear hair cells. *Proc. R. Soc. Lond.* B. **248**, 215–221.

Hackney, C. M., Furness, D. N. & Mahendrasingam, S. 1993 The mechanotransduction channels in cochlear hair cells may be revealed by antibodies which recognise other amiloride-sensitive channels. In *Biophysics of hair cell sensory systems* (ed. H. Duifhuis, J. W. Horst, P. van Dijk & S. M. van Netten), pp. 107–115 Singapore, World Scientific.

Howard, J., Roberts, W. M. & Hudspeth, A. J. 1988 Mechanoelectrical transduction by hair cells. *Ann. Rev. Biophys. Biophys. Chem.* **17**, 99–124

Jacobs, R. A. & Hudspeth, A. J. 1990 Ultrastructural correlates of mechanoelectrical transduction in hair cells of the bullfrog's internal ear. *Cold Spring Harbor symposium on quantitative biology* **55**, 547–561.

Jiang, D., Furness, D. N., Hackney, C. M. & Lopez, D. E. 1993 Microslicing of the resin-embedded cochlea in comparison with the surface preparation technique for analysis of hair-cell number and morphology. *Brit. J. Audiol.* **27**, 195–203.

Lim, D. J. 1986 Functional structure of the organ of Corti. *Hear. Res.* **22**, 117–146.

Osborne, M. P., Comis, S. D. & Pickles, J. O. 1984 Morphology and cross-linkage of stereocilia in the guinea-pig labyrinth examined without the use of osmium as a fixative. *Cell Tiss. Res.* **237**, 43–48.

Pickles, J. O. 1993 A model for the mechanics of the stereociliar bundle on acousticolateral hair cells. *Hear. Res.* **68**, 159–172.

Zetes, D. E. 1995 Mechanical and morphological study of the stereocilia bundle in the mammalian auditory system, Ph.D. Thesis, Stanford University.

Received 11 July 1996; accepted 13 August 1996